Seasonal and interannual variations in Antarctic backscatter signature from 2000 to 2006 as observed by QuikSCAT

Ben Lambert and David Long
Brigham Young University, 459 Clyde Building, Provo, UT 84602

1. ABSTRACT

Time-series analysis of Antarctic QuikSCAT data reveals several trends. An annual seasonal cycle in which backscatter power increases during the Austral winter and decreases during the Austral summer, is observed over most of the continent, with varying magnitude. Several areas also show a large ($\sim$ 10dB) decrease in average backscatter during the Austral summer, suggesting melt events. As expected, seasonal variations are strongly dependent on latitude; the southernmost observable portion of the continent is much less seasonably variable than the coasts. Interanual trends show strong long-term trends superimposed on seasonal cycles in much of the continent. Along the coast of most of the continent, backscatter has consistently increased, on the order of 0.5 dB/year, during the seven-year study period. Other regions, mostly in the West-Antarctic interior show the opposite trend, with average backscatter decreasing on the order of 0.5 dB/year.

2. INTRODUCTION

Previous studies have established that the Antarctic ice sheet is an important factor in local and global climate patterns, and that the nature of the ice sheet may be changing. Thus, it is important to understand the nature of variations in the Antarctic ice sheet. Space-borne microwave-frequency scatterometers are an ideal tool for this sort of large-scale application.

The general methodology we follow is similar to that of Bingham and Drinkwater in [**??**]. The instruments they used were the C-band scatterometer EScat, the Ku-band scatterometers NSCAT and Seasat and the multichannel radiometer SSM/I, during a study period from 1992 to 1997. Our study uses data only from the Ku-Band scatterometer SeaWinds on QuikSCAT, and our study period is 2000-2006 inclusive.

3. DESCRIPTIVE MODEL

To create a consistent data set, we bin L1B observations spatially and temporally. Each bin corresponds to a 4-day 10 pixel by 10 pixel average, where a pixel is defined by the scatterometer image reconstruction (sir) algorithm (see [**??**]). A simple descriptive model represents normalized backscatter power (σ^0) as a function of azimuth angle relative to north (ϕ), and the model is applied individually to each data bin [**??**],

$$\sigma^0(\phi) = A_0 + \sum_{k=1}^{4} A_k \cos(k\phi) + B_k \sin(k\phi). \tag{1}$$

Incidence angle terms are excluded because of QuikSCAT's dual-pol, fixed incidence angle observation geometry. Model coefficients are determined by ordinary least squares linear regression. From these model coefficients we extract the k^{th} order modulation magnitude, $M_k = \sqrt{A_k^2 + B_k^2}$, and phase, $\chi_k = \tan^{-1}(\frac{B_k}{A_k})$. As an example, Figure 1 shows L1B data from 1 bin in East-Antarctica for Julian Day 321-324, 2005, where the data has been further binned into four degree azimuth bins.

The parameters that are of most interest in this study are the average normalized cross-section backscatter power (M_0), and the even (real) magnitude and phase terms (M_2, M_4, χ_2, χ_4).

Magnitude parameters (Figure 2) are related to scattering properties, such as local incidence angle (surface slope), reflectivity, and absorption. The topographical features that influence modulation magnitude are the composition of the ice and snow sheets, layering effects, and the presence and size of sastrugi and dunes. Phase parameters (Figure 3) are influenced by the orientation of these features, which is often closely related to the direction of katabatic wind. For instance, sastrugi, which are erosional features, tend to be aligned with wind

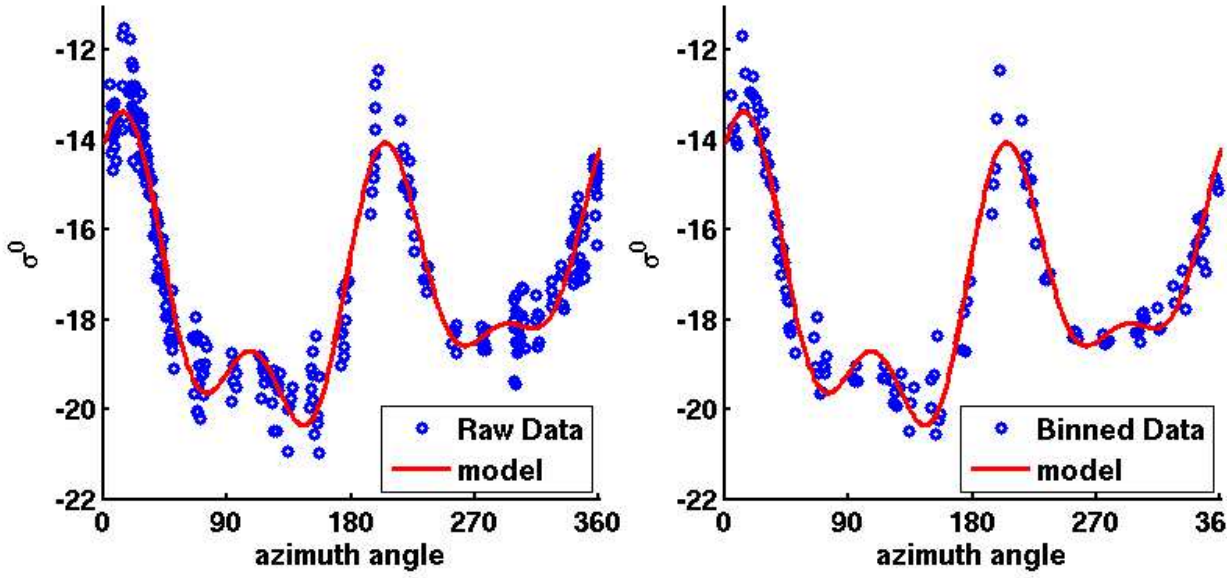

Figure 1. L1B data from a single East-Antarctic bin with superimposed model. Left) Raw data. Right) Data in azimuth bins.

Table 1. Model coefficient and modulation parameter values for the data shown in Figure 1

coefficient	value	coefficient	value	parameter	value	parameter	value
A_0	-17.37			M_0	-17.37		
A_1	0.70	B_1	-0.72	M_1	1.00	χ_1	-45.82
A_2	1.74	B_2	1.48	M_2	2.29	χ_2	40.38
A_3	0.48	B_3	-0.37	M_3	0.61	χ_3	-37.73
A_4	0.26	B_4	1.21	M_4	1.23	χ_4	78.97

direction, while dunes, which are depositional features, tend to be aligned perpendicular to the wind direction [**??**]. The holes in the centers of the images in Figures 2 and 3 represent the southern extent of sufficiently dense QuikSCAT observations.

Long and Drinkwater ([**??**]) show that first and second harmonic terms are necessary to properly capture the backscatter signature produced by common Antarctic topographical features, such as dunes and sastrugi. We find that QuikSCAT's dense azimuth sampling reveals additional backscatter features suggesting a fourth order model is more appropriate in this application. To demonstrate the necessity of a higher order model, we consider residual variance as a measure of goodness of fit. Figure **??** displays how adding the third and fourth harmonic to our model changes this quantity. Much of the analysis in this report focuses on temporal changes at lower latitudes, including the Antarctic peninsula, and in Eastern Antarctica, exactly those places where the difference in model performance is greatest. We find that increasing the model order beyond four scarcely improves performance.

4. MAGNITUDE CHANGES

Following the methods used in [**??**], we plot the three magnitude parameters of interest (M_0, M_2, and M_4, phase parameters are addressed in the next section) pixel-by-pixel as a time series covering the seven year study period. We remove the average yearly cycle and plot the resulting anomaly data. We fit a simple sinusoidal model to the average yearly cycle,

$$Y(t) = \alpha \cos(2\pi t - t_0) + \eta_Y, \tag{2}$$

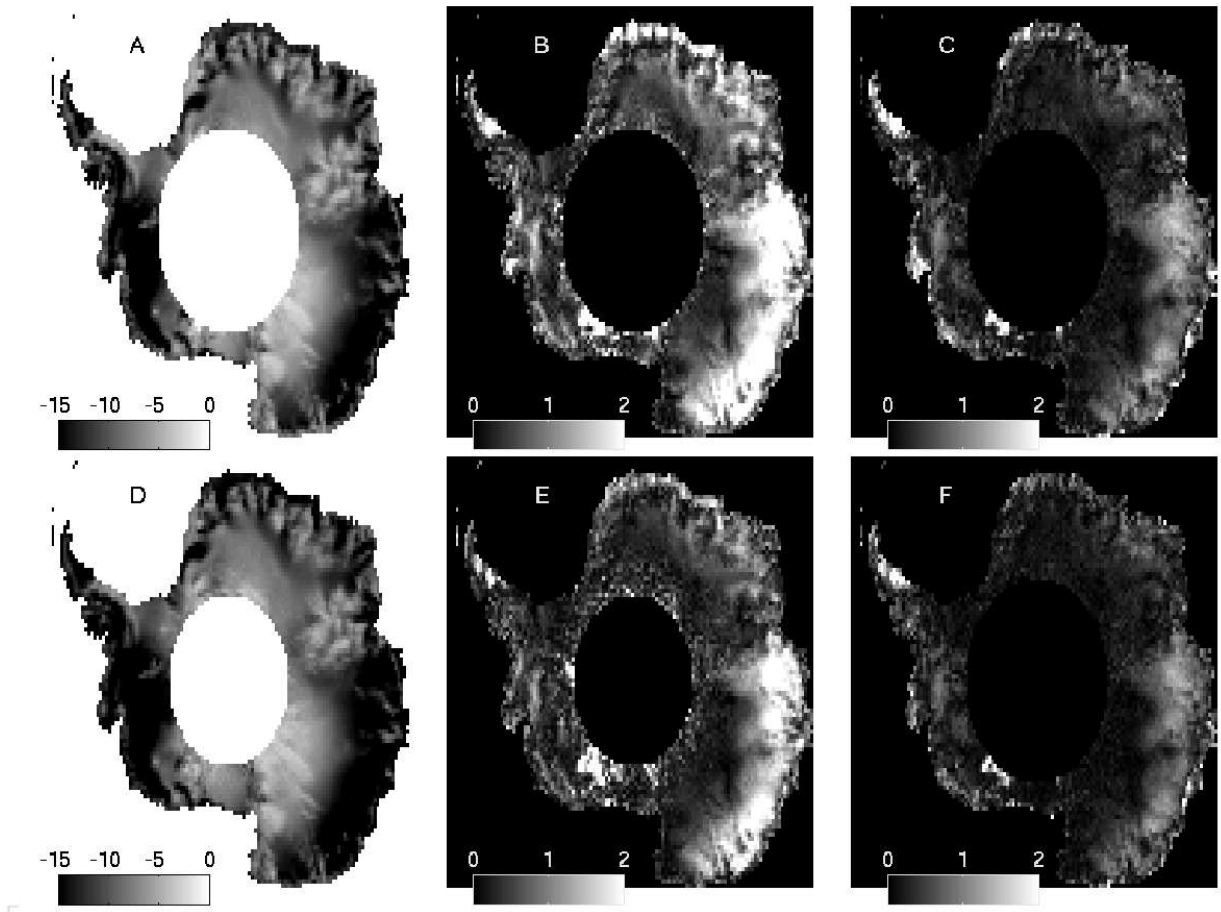

Figure 2. Magnitude images, all units dB. A) M_0 H-pol. B) M_2 H-pol. C) M_4 H-pol. D) M_0 V-pol. E) M_2 V-pol. F) M_4 V-pol.

where α and t_0 summarize the magnitude and phase, respectively, of the cyclical data. For the anomaly data we remove short-term effects with a 91 point (one year) low-pass filter, and fit a simple linear model,

$$A(t) = C + Dt + \eta_A, \tag{3}$$

where C and D represent the intercept and slope, respectively. In both models η is the residual term. We make no assertion that these models represent more than the crudest summary of trends in the data.

In the following sections we apply this method to M_0, M_2, and M_4 data from several interesting locations throughout the continent (Figure 4). In all instances, pixels are chosen to be some distance from the coast. Only V-pol data is displayed, as H-pol data yields similar results.

4.1 Average normalized backscatter, M_0, trends

Average normalized backscatter, M_0, is the most important, and most variable, modulation parameter. When controlled for incidence angle effects, backscatter from ice sheets is well-modeled as a function of grain radius, firn density, and dielectric constant of the ice grains within the sheet [**??**], all of which are influenced by air and firn temperature, and accumulation.

Time series, yearly cycle, and anomaly M_0 data for locations A-G are displayed in Figure 5, with corresponding change parameter values, α and D, recorded in Table 2. These locations were chosen to display a variety of features. One notices a sharp "reset" behavior around the year boundary in several of the locations. This

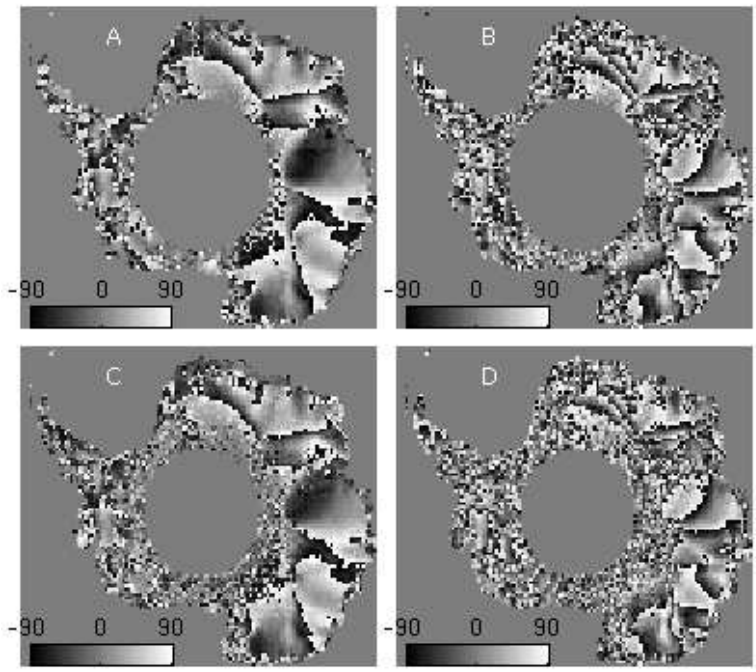

Figure 3. Phase images, all units degrees relative to north. A) χ_2 H-pol. B) χ_4 H-pol. C) χ_2 V-pol. D) χ_4 V-pol.

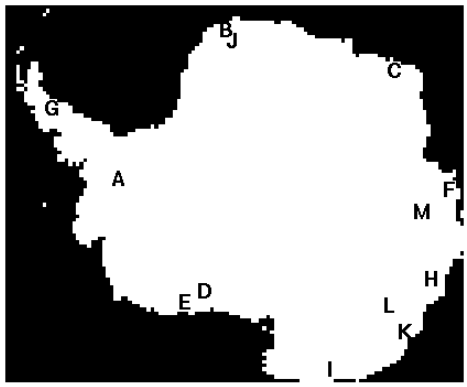

Figure 4. Map of the locations for which data in plotted in Figures 5, 6, and 7.

signature is commonly associated with a melt/refreeze cycle, as water is much less reflective than ice, especially at oblique incidence.

As expected, the nature of these melt events corresponds to latitude, with the more northern locations, B and G, experiencing longer and more severe melt events than the other locations. The severe backscatter decrease during the 2005-2006 year boundary in locations D and E corresponds to a known melt event in the Ross Ice Shelf [**??**]. The observed backscatter increases after melt events in all locations except D, which shows a small, consistent decrease in backscatter, and location G, which tends to remain constant. Backscatter in location A shows not melt events, but has a strong negative trend, perhaps as he result dampening due to accumulation.

4.2 Second and fourth order modulation magnitude, M_2 and M_4, trends.

The same methods are applied to M_2 and M_4 V-pol data for three interesting locations - map locations H-J for M_2 data, locations K-M for M_4 data - and the results are presented in Figures 6 and 7, with corresponding

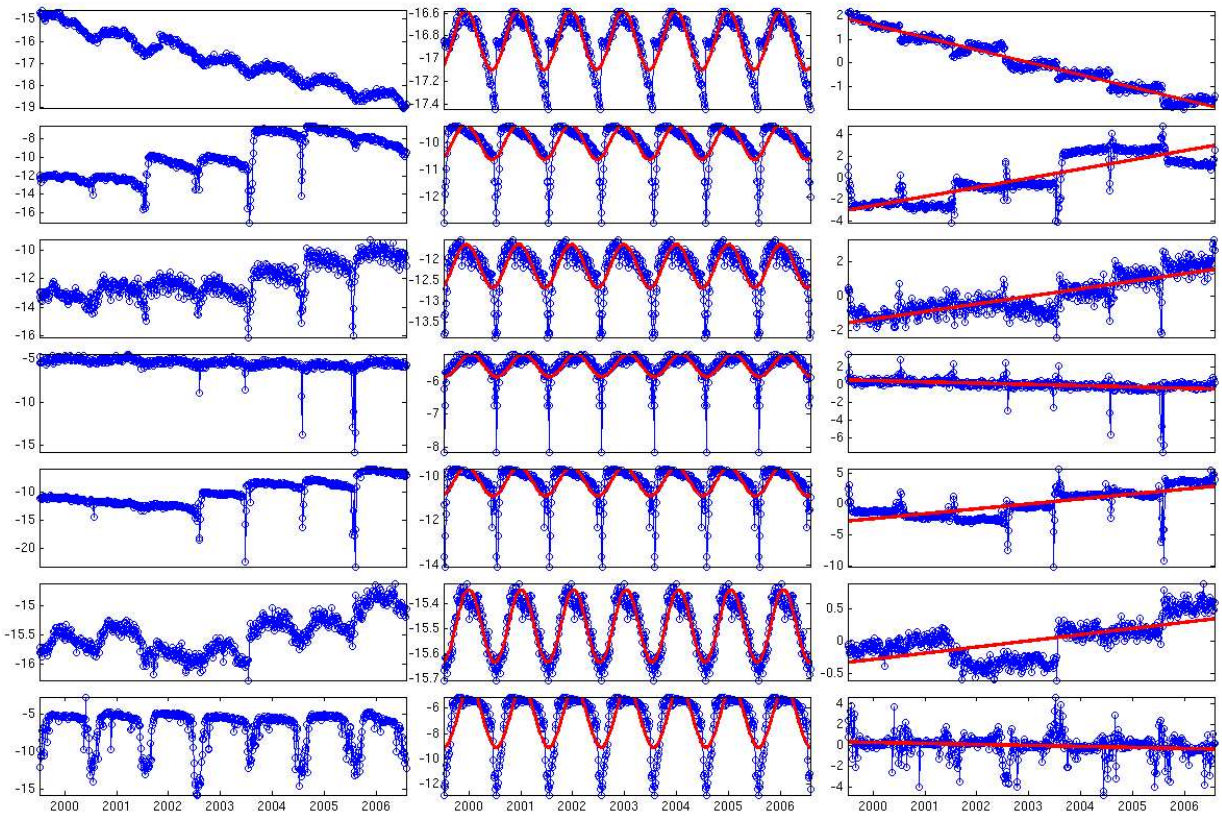

Figure 5. Time series data (left column), average yearly cycle (middle column) and filtered anomaly data (right column) for locations A-G, from top to bottom.

Table 2. Values of α, in dB, and D, in dB/year, for M_0 data from locations A-G.

location	α	D	location	α	D
A	0.26	-.054	E	0.66	-0.80
B	0.64	-0.86	F	0.15	0.01
C	0.51	0.44	G	2.36	-0.01
D	0.35	-0.14			

change parameter values, α and D, recorded in table 3. Seasonal cycles are clear in both data sets, but anomaly data trends are either too variable, in the M_2 case, or two small, in the M_4 case, to be telling.

Table 3. Values of α, in dB, and D, in dB/year, for M_2 and M_4 data from locations H-J and K-M respectively.

M_2			M_4		
location	α	D	location	α	D
H	0.13	-8.4e-4	K	0.07	-5.9e-4
I	0.11	5.9e-4	L	0.03	1.7e-4
J	0.08	-7.5e-4	M	0.02	-1.0e-4

4.3 Composite Change Images

We perform the same analysis on every pixel within an Antarctic landmask for all three modulation magnitude parameters at both polarizations and present D images in Figure 8, α images for M_0 data at both polarizations are presented in Figure 9. Inspection of these images reveals several interesting trends. The D images reveal strong spatial coherence, especially for M_0, in which the coastal regions show an increase in backscatter, with an exception of the Antarctic peninsula which, along with West-Antarctica, shows a predominately increasing

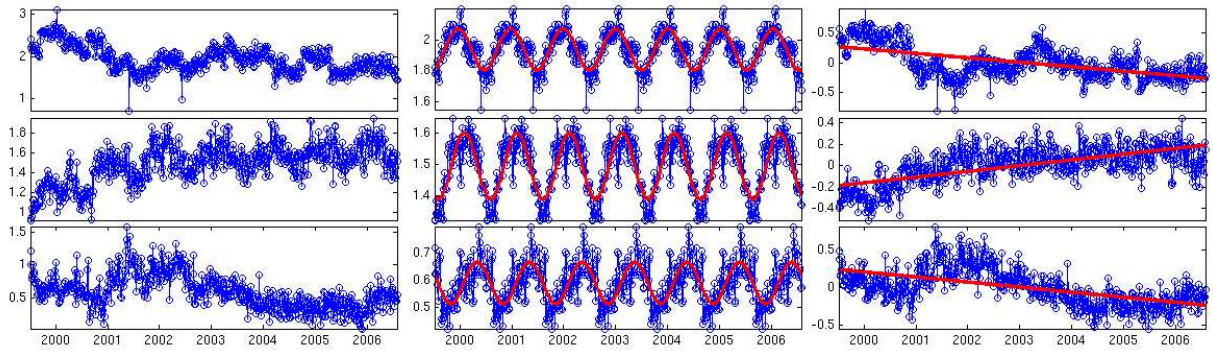

Figure 6. Time series data (left column), average yearly cycle (middle column) and filtered anomaly data (right column) for M_2 data from locations H-J, from top to bottom.

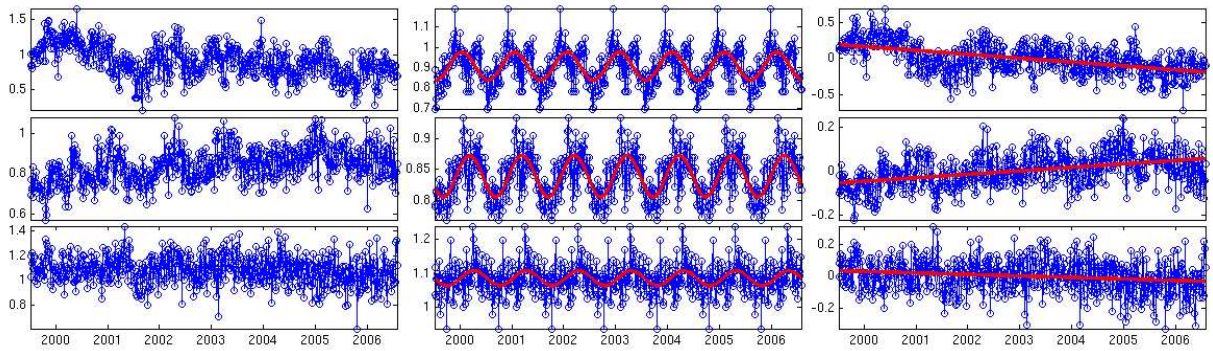

Figure 7. Time series data (left column), average yearly cycle (middle column) and filtered anomaly data (right column) for M_4 data from locations K-M, from top to bottom.

backscatter. M_2 data shows a predominately decreasing trend in eastern Antarctica. Trends in the M_4 data are also spatially coherent, and predominantly negative, but small.

Images of α also show an interesting, if expected, pattern of significant seasonal cycles appearing only in a ring of northernly locations around the perimeter of the continent. The rest of the continent, despite some spatial coherence, shows almost no seasonal variations. This sharp distinction between portions of the continent appears to demarcate where summer melting regularly occurs and where it does not.

4.4 Control

To ensure that the trends observed result from actual changes in the scattering properties of the ice sheet we present two controls (see Figure 11). First, to ensure that QuikSCAT's instrumentation has remained calibrated during the seven-year study period we present a M_0 time series data for an extremely southern target, where it is reasonable to assume that air and firn temperature experience little, if any, seasonal variation. Indeed, we observe no seasonal or interanual variations in backscatter at this location.

Second, to ensure that there have been no long-term changes in QuikSCAT's observation geometry we present time series data of average incidence angle and average azimuth angle for observations at location A. average azimuth angle is highly variable, but shows no long-term trend that could account for the consistently changing backscatter observed at location A. Incidence angle does show two superimposed trends, but of such small magnitude (~ 0.03 degrees) that they could not possible account for any significant change in observed backscatter.

5. MODEL PHASE PARAMETER CHANGES

Model phase parameters (χ_2, χ_4) reflect the orientation of scattering targets on the surface and layers within the ice sheet. These scatterers, in turn, are created by the continental katabatic wind regime, and have been shown to be useful indicators of prevailing wind direction [**??**], with peaks in azimuth modulation corresponding

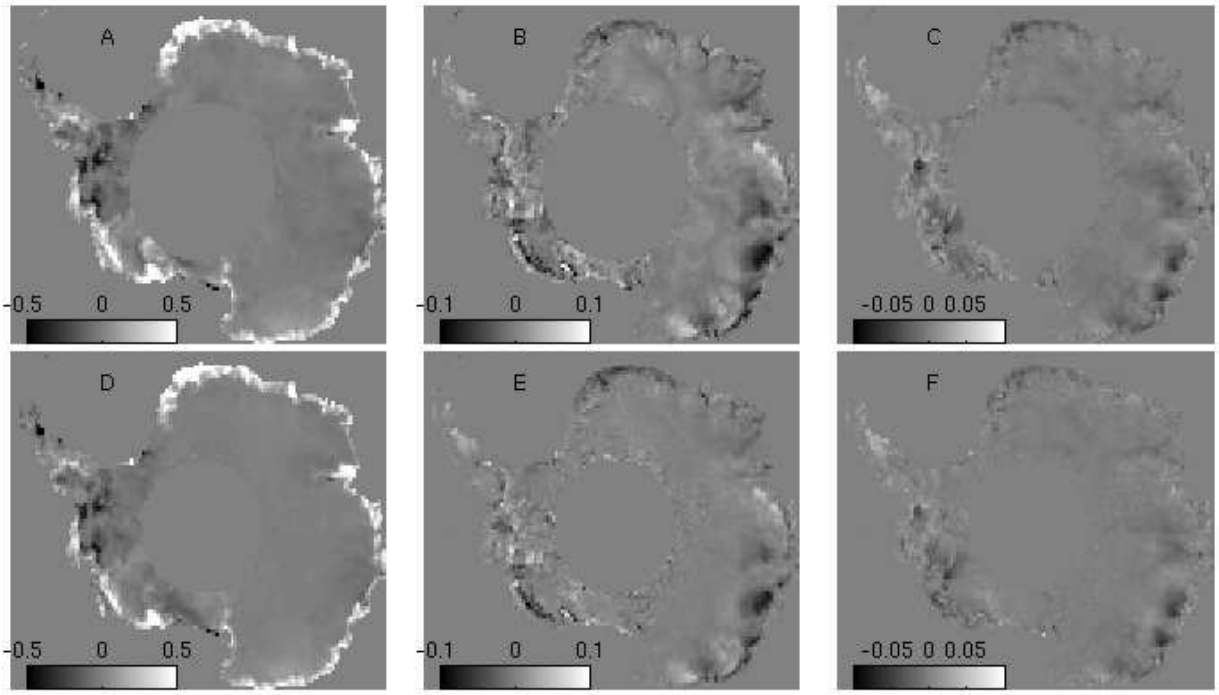

Figure 8. Values of D, dB/year, for A) H-pol M_0. B) H-pol M_2, C) H-pol M_4, D) V-pol M_0, E) V-pol M_2, F) V-pol M_4.

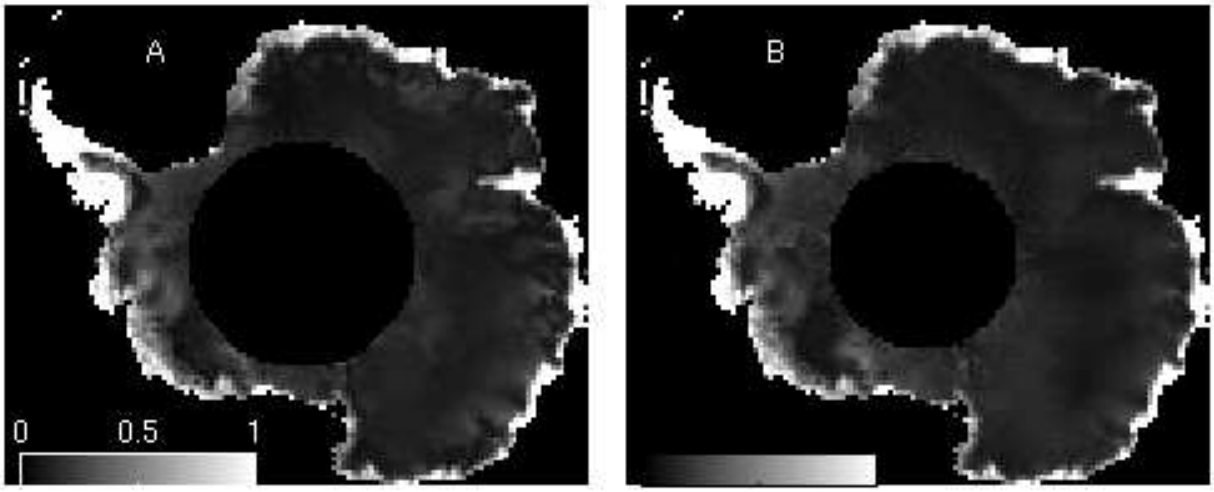

Figure 9. Pixel-wise values of α in dB. A) M_0, H-pol data, B) M_0, V-pol data.

to the up and down wind directions [**??**]. Antarctic katabatic wind has been shown to have consistent velocity and orientation for extended periods of time [**??**], therefore, changes in azimuth modulation phase parameters would indicate a changed scattering regime, possible resulting from a changed wind orientation.

Figures of the difference in phase parameters from austral summer 2000 to austral summer 2006 (see Figure 12) show little coherent change. What change does appear takes the form of "salt and pepper" noise, with values near $\pm 180^{0}$, probably as a result of upwind/downwind ambiguity. An example of this can be seen in Figure 1, where the two highest peaks, and even the two secondary peaks, are about 180^{0} degrees apart. It is precisely this "jumpy" character of phase parameter change that prevents us from using the change modeling techniques that worked well with magnitude parameters. In general, these results suggest that there is little significant change in the Antarctic katabatic wind regime during the study period.

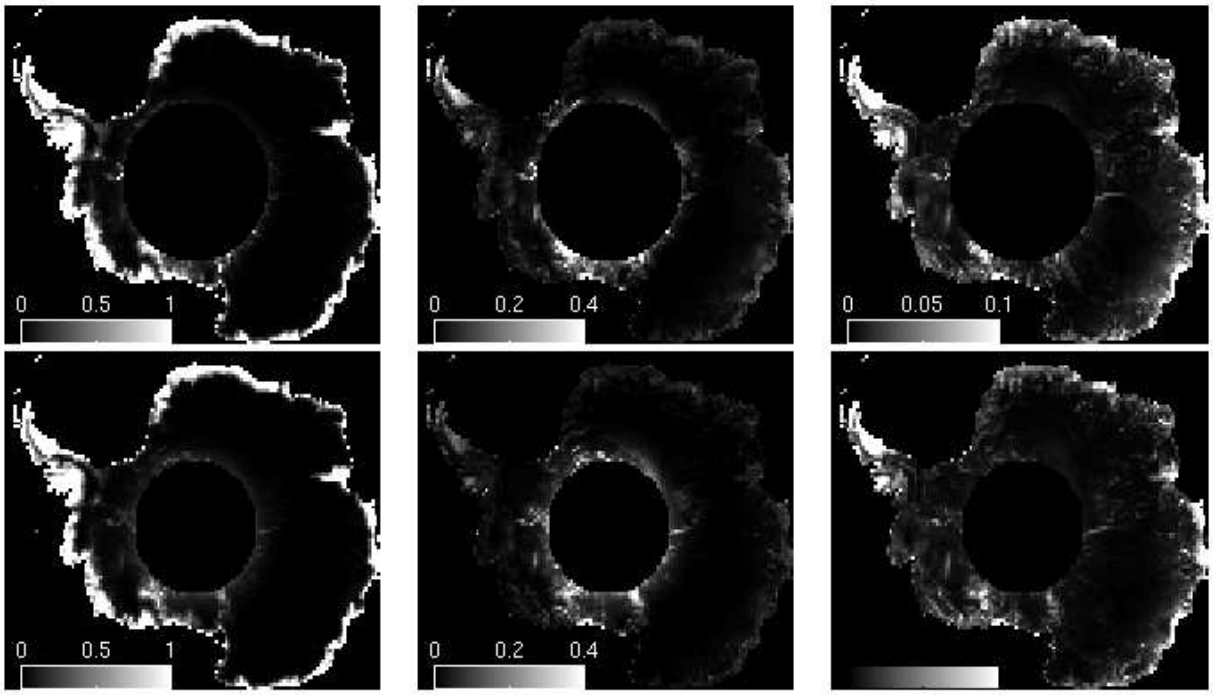

Figure 10. Variance of η_A, dB^2, for A) H-pol M_0. B) H-pol M_2, C) H-pol M_4, D) V-pol M_0, E) V-pol M_2, F) V-pol M_4.

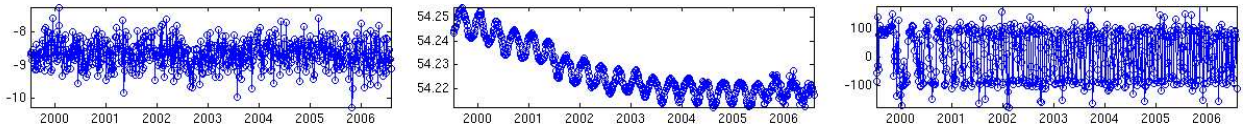

Figure 11. Control Variables. Left) M_0 time series for an extreme southern target. Center) Average incidence angle time series at location A. Right) Average azimuth angle time series at location A.

6. SUMMARY AND CONCLUSION

Motivated by the importance of the Antarctic ice sheet in global climate models, we have presented a cataloging of certain parameters the Antarctic ku-band backscatter signature as observed by QuikSCAT from 2000-2006. Significant results are the observation of consistently increasing average backscatter power along much of the Antarctic coast, and the consistently decreasing backscatter power in West-Antarctica.

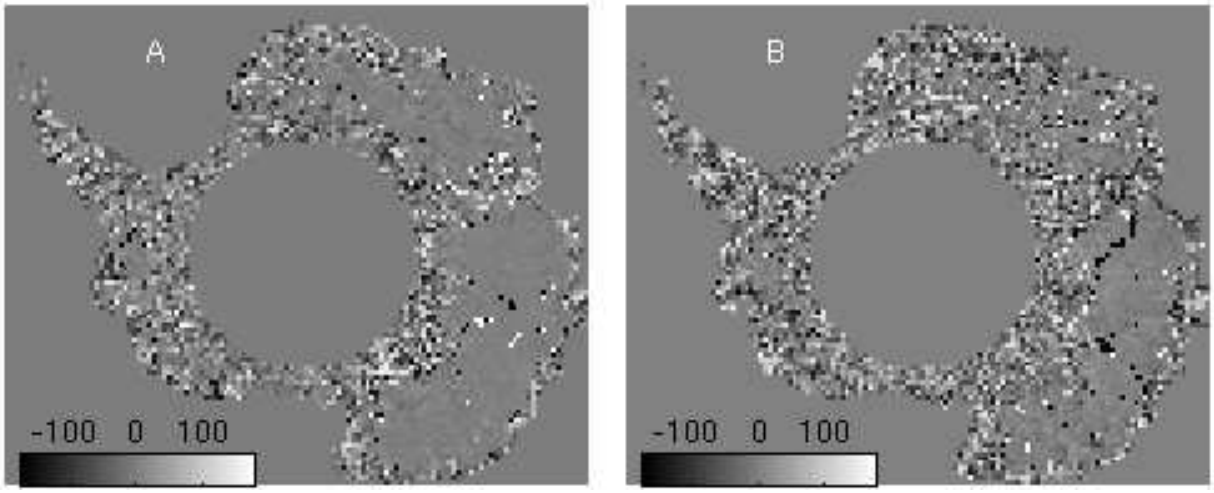

Figure 12. Difference images: Julian Day 1-4 2000 and Julian Day 1-4 2006. A) M_2, B) M_4.